Eur. Phys. J. B **25**, 345–350 (2002)
DOI: 10.1140/epjb/e20020039

THE EUROPEAN PHYSICAL JOURNAL B
EDP Sciences

Directed transport of an asymmetric particle pair induced by non-equilibrium conditions

M. Porto[a]

Max-Planck-Institut für Physik komplexer Systeme, Nöthnitzer Strasse 38, 01187 Dresden, Germany

Received 17 August 2001 and Received in final form 11 October 2001

Abstract. The hopping motion of a classical bounded pair of two particles along a chain is investigated. It is shown that in the asymmetric case of the system dynamics including excited states which differ from the respective ground states by the barrier to be overcome by one of the two particles, the over- and underpopulation of these excited states leads to a directed motion of the particle pair. Thereby, overpopulation results in one direction of motion, whereas underpopulation results in the opposite direction, and the mean velocity is determined by the amount of over-resp. underpopulation. For small deviations from equilibrium, the system exhibits linear response well known from other ratchet-type models. Possible generalizations and applications are discussed.

PACS. 05.60.Cd Classical transport – 05.40.−a Fluctuation phenomena, random processes, noise, and Brownian motion – 87.16.Nn Motor proteins

1 Introduction

Despite that the handling and manipulation of individual atoms and molecules has become widespread in many fields of science [1], the important challenge has still remained to further 'tame' them and make nanoscale objects perform useful mechanical functions. While first steps in the direction towards molecular machinery have already been taken experimentally [2], specifically the investigation of how to transform the supplied energy in an efficient and controllable way to a specific function on the molecular scale is still at its beginning. Much of the theoretical research in this area has focused on the case of the function to be performed being directed transport. In particular, the motion of particles in ratchet potentials without spatial symmetry under the influence of stochastic and/or periodic forces has been intensively discussed, both in terms of Newton-/Langevin-type equations of motion [3] or focusing on hopping models [4], partly motivated by possible applicability to biological motors [5]. Having the construction of man-made molecular motors in mind, one would like to establish concepts which allow for the local or internal conversion of the supplied energy to directed motion. For example, in so-called n-state ratchets, the switching between the different potentials the particle is subject to can also be considered as induced by driven changes between internal states of the particle, thus providing a local or internal conversion of the supplied energy. Another possibility is given by systems consisting of two coupled particles, for example two identical particles in an on/off-ratchet [6] or in a static ratchet potential using a time-dependent inter-particle coupling [7], as well as two particles which differ by their frictional behavior [8] or simply by their mass [9]. It is preferable to develop more concepts in this direction, which may either be along the lines of the ones outlined above or may rely on different mechanisms such as some recently proposed alternative concepts [10].

The aim of this work is to study a hopping model of a coupled particle pair which covers and combines several aspects of the before-mentioned continuous two particle models [6–9]. To be specific, the hopping motion of a classical bounded pair of two particles along an equipotential chain is investigated in the asymmetric case of the system dynamics including excited states which differ from the respective ground states by the barrier to be overcome by one of the two particles. Analogously to previous models, bringing the system into non-equilibrium by over- and underpopulating these excited states leads to a directed motion of the particle pair. Thereby, overpopulation results in one direction of motion, whereas underpopulation yields the opposite direction, and the mean velocity is determined by the amount of over- resp. underpopulation, with the system exhibiting a linear response regime for small deviations from equilibrium [11]. The motivation to study this model is two-fold: On the one hand, it might be considered as a simple discretized version of the corresponding Langevin description in the overdamped limit, providing an intuitive physical picture of particles stochastically moving between sites relevant for microscopic transport processes [12]. Additionally, in difference to continuous descriptions, the Markovian nature of hopping models allows

[a] e-mail: porto@mpipks-dresden.mpg.de

a general discussion in the context of distinct system states and transitions between them, making hopping systems in general of broader applicability beyond directed transport. This point is readdressed in the Conclusions towards the end.

2 Model

In the system under consideration, there are two particles located on a one-dimensional equipotential chain, the left and right one labelled 1 and 2, respectively. The pair is coupled in the sense that the two particles either sit on nearest neighboring sites, or that they are separated by a maximum of one site in between, but not further apart. There is, however, no further interaction between them. One can easily convince oneself that to map this system on distinct states under the restrictions that (i) two states are connected by not more than one transition, and that (ii) each transition corresponds to a specific particle hop, one needs a minimum of four distinct states. These four states are called further on $\sigma_{\mathcal{A}}$, $\sigma_{\mathcal{B}}$, $\sigma_{\mathcal{C}}$, and $\sigma_{\mathcal{D}}$. There are the two states $\sigma_{\mathcal{A}}$ and $\sigma_{\mathcal{C}}$, characterized by the particles sitting on nearest neighboring sites, as well as the two states $\sigma_{\mathcal{B}}$ and $\sigma_{\mathcal{D}}$, characterized by the two particles being separated by one site, see Figure 1. In the following, it is assumed that (i) the system can become excited when the two particles are on nearest neighboring sites, leading to two additional excited states $\sigma^\star_{\mathcal{A}}$ and $\sigma^\star_{\mathcal{C}}$ which differ in potential energy by an energy difference ϵ when compared to the four equipotential states $\sigma_{\mathcal{A}}$, $\sigma_{\mathcal{B}}$, $\sigma_{\mathcal{C}}$, and $\sigma_{\mathcal{D}}$. The two excited states $\sigma^\star_{\mathcal{A}}$ and $\sigma^\star_{\mathcal{C}}$ can be reached, analogously to the states $\sigma_{\mathcal{A}}$ and $\sigma_{\mathcal{C}}$, from the states $\sigma_{\mathcal{B}}$ or $\sigma_{\mathcal{D}}$ by a transition corresponding to a particle hop, or by direct transitions from the states $\sigma_{\mathcal{A}}$ or $\sigma_{\mathcal{C}}$ which do not involve a particle hop, *cf.* Figure 1a. As shown below, the latter two additional transitions not involving a particle hop do neither alter the symmetry nor the equilibrium behavior of the system, but introduce a simple manner of feeding energy into the system by allowing to 'pump' these two transitions. In addition to the existence of the excited states it is assumed that (ii) they differ from the respective ground states by the barrier particle 2 has to overcome when leaving or entering the excited states, thus breaking the spatial symmetry in a ratchet-type manner.

To exemplify the relation between the change in system state and the motion of the two particles, in Figure 1b shown are six representative examples of particle motion. In all cases, it is assumed that the system is in state $\sigma_{\mathcal{A}}$ at the beginning, with both particles sitting on nearest neighboring sites. It should be noted that due to symmetry, analogous examples can be constructed by exchanging simultaneously $\sigma_{\mathcal{A}} \rightleftarrows \sigma_{\mathcal{C}}$, $\sigma^\star_{\mathcal{A}} \rightleftarrows \sigma^\star_{\mathcal{C}}$, and $\sigma_{\mathcal{B}} \rightleftarrows \sigma_{\mathcal{D}}$.

In example (i), $\sigma_{\mathcal{A}} \stackrel{1}{\rightarrow} \sigma_{\mathcal{B}} \stackrel{1}{\rightarrow} \sigma_{\mathcal{A}}$ (the numbers above the arrows indicate which particle moves during the transition), particle 1 hops away from particle 2 to the left, overcoming the barrier $\Delta \geq 0$ (for the actual transition rates see below, left and right refers here and in the following to the particles' spatial motion), which brings the system to state $\sigma_{\mathcal{B}}$. Afterwards, particle 1 hops back to the right, surmounting the same barrier Δ, which brings the system back to state $\sigma_{\mathcal{A}}$. In example (ii), $\sigma_{\mathcal{A}} \stackrel{2}{\rightarrow} \sigma_{\mathcal{D}} \stackrel{2}{\rightarrow} \sigma_{\mathcal{A}}$, particle 2 hops away from particle 1 to the right, overcoming the barrier Δ, which brings the system to state $\sigma_{\mathcal{D}}$. Similar to example (i), particle 2 hops back to the left in the next step, surmounting the same barrier Δ, which

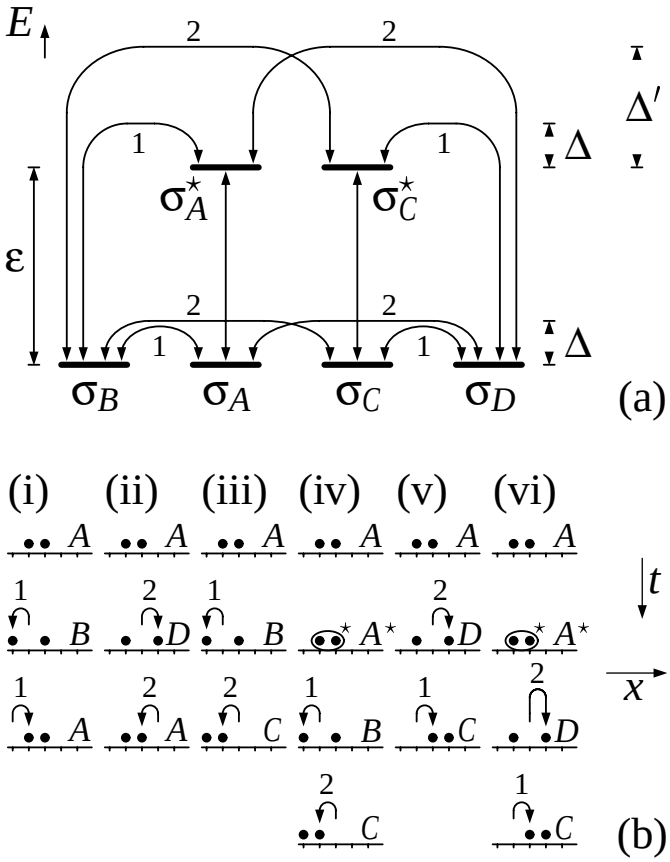

Fig. 1. (a) Sketch of the four states $\sigma_{\mathcal{A}}$, $\sigma_{\mathcal{B}}$, $\sigma_{\mathcal{C}}$, and $\sigma_{\mathcal{D}}$ and the two excited states $\sigma^\star_{\mathcal{A}}$, and $\sigma^\star_{\mathcal{C}}$, as well as the respective transitions with the barriers Δ and Δ' and the energy difference ϵ. The vertical axis indicates the potential energy, and as an example the case $\epsilon > 0$ and $\Delta' > \Delta$ is shown. The number at the transition arrows indicate which particle is moving during the respective transition. (b) Six representative examples of particle motion in relation to the change in system state, all starting with the system being in state $\sigma_{\mathcal{A}}$. The examples show snapshots of the particles' position, and the arrows indicated which particle motion lead to the respective current system state, the latter named on the right site of the snapshot. In the two examples (iv) and (vi), the system passes through the excited state $\sigma^\star_{\mathcal{A}}$, indicated by * in the figure. In all examples, both particle 1 and 2 surmount the barrier Δ during their hops, with the exception of one hop in the last example (vi), during which particle 2 overcomes the different barrier Δ' in the step $\sigma^\star_{\mathcal{A}} \stackrel{2}{\rightarrow} \sigma_{\mathcal{D}}$, indicated by the larger arrow. It should be noted that due to symmetry, analogous examples can be constructed by exchanging simultaneously $\sigma_{\mathcal{A}} \rightleftarrows \sigma_{\mathcal{C}}$, $\sigma^\star_{\mathcal{A}} \rightleftarrows \sigma^\star_{\mathcal{C}}$, and $\sigma_{\mathcal{B}} \rightleftarrows \sigma_{\mathcal{D}}$.

brings the system back to state $\sigma_{\mathcal{A}}$. In both examples, the whole pair does not gain any distance.

This is in difference to the last four examples, in which the whole pair moves one step to the left, as in examples (iii) and (iv), or to the right, as in example (v) and (vi). The direction of motion depends whether particle 1 hops before particle 2 (step to the left) or inversely particle 2 hops before particle 1 (step to the right). In example (iii), $\sigma_{\mathcal{A}} \stackrel{1}{\rightarrow} \sigma_{\mathcal{B}} \stackrel{2}{\rightarrow} \sigma_{\mathcal{C}}$, by a hop of particle 1 to the left, the system changes from state $\sigma_{\mathcal{A}}$ to state $\sigma_{\mathcal{B}}$ as in the first step of example (i). In difference to example (i), in the next step particle 2 follows its predecessor and hops to the left, overcoming barrier Δ, which brings the system to state $\sigma_{\mathcal{C}}$. In example (iv), $\sigma_{\mathcal{A}} \rightarrow \sigma^{\star}_{\mathcal{A}} \stackrel{1}{\rightarrow} \sigma_{\mathcal{B}} \stackrel{2}{\rightarrow} \sigma_{\mathcal{C}}$, the system first changes to the excited state $\sigma^{\star}_{\mathcal{A}}$ without a particle hop, after which particle 1 and then particle 2 hop to the left, both overcoming barrier Δ as in example (iii), which brings the system *via* state $\sigma_{\mathcal{B}}$ to state $\sigma_{\mathcal{C}}$. It is important to note that particle 1, despite that its hop occurs when the system is in the excited state $\sigma^{\star}_{\mathcal{A}}$, has to surmount the same barrier Δ as when the system was in state $\sigma_{\mathcal{A}}$. In example (v), $\sigma_{\mathcal{A}} \stackrel{2}{\rightarrow} \sigma_{\mathcal{D}} \stackrel{1}{\rightarrow} \sigma_{\mathcal{C}}$, by a hop of particle 2 to the right, the system changes from state $\sigma_{\mathcal{A}}$ to state $\sigma_{\mathcal{D}}$ as in the first step of example (ii). In difference to example (ii), in the next step particle 1 follows its predecessor and hops to the right, overcoming barrier Δ, which brings the system to state $\sigma_{\mathcal{C}}$. In the last example (vi), $\sigma_{\mathcal{A}} \rightarrow \sigma^{\star}_{\mathcal{A}} \stackrel{2}{\rightarrow} \sigma_{\mathcal{D}} \stackrel{1}{\rightarrow} \sigma_{\mathcal{C}}$, the system first changes to the excited state $\sigma^{\star}_{\mathcal{A}}$ without a particle hop, after which particle 2 and then particle 1 hop to the right. As the hop of particle 2 occurs when the system is in an excited state, in this case $\sigma^{\star}_{\mathcal{A}}$, it has to surmount the different barrier $\Delta' \geq 0$, as indicated by the larger arrow in Figure 1b, whereas afterwards particle 1 has to overcome barrier Δ as in the examples before.

The actual transition rates connecting pairwise the six system states can be directly read off from Figure 1a. For example, for states on the same potential energy such as $\sigma_{\mathcal{A}}$ and $\sigma_{\mathcal{B}}$, the interconnecting transition rates are given by $\Gamma_{\sigma_{\mathcal{A}}\rightarrow\sigma_{\mathcal{B}}} = \exp[-\Delta/(k_{\mathrm{B}}T)]$ and $\Gamma_{\sigma_{\mathcal{B}}\rightarrow\sigma_{\mathcal{A}}} = \exp[-\Delta/(k_{\mathrm{B}}T)]$, so that detailed balance $\Gamma_{\sigma_{\mathcal{B}}\rightarrow\sigma_{\mathcal{A}}}/\Gamma_{\sigma_{\mathcal{A}}\rightarrow\sigma_{\mathcal{B}}} = 1$ is fulfilled. For states on different potential energies such as $\sigma_{\mathcal{B}}$ and $\sigma^{\star}_{\mathcal{A}}$ or $\sigma_{\mathcal{B}}$ and $\sigma^{\star}_{\mathcal{C}}$, the interconnecting transition rates for $\epsilon > 0$ are $\Gamma_{\sigma_{\mathcal{B}}\rightarrow\sigma^{\star}_{\mathcal{A}}} = \exp[-(\epsilon + \Delta)/(k_{\mathrm{B}}T)]$ and $\Gamma_{\sigma^{\star}_{\mathcal{A}}\rightarrow\sigma_{\mathcal{B}}} = \exp[-\Delta/(k_{\mathrm{B}}T)]$ as well as $\Gamma_{\sigma_{\mathcal{B}}\rightarrow\sigma^{\star}_{\mathcal{C}}} = \exp[-(\epsilon + \Delta')/(k_{\mathrm{B}}T)]$ and $\Gamma_{\sigma^{\star}_{\mathcal{C}}\rightarrow\sigma_{\mathcal{B}}} = \exp[-\Delta'/(k_{\mathrm{B}}T)]$, so that $\Gamma_{\sigma_{\mathcal{B}}\rightarrow\sigma^{\star}_{\mathcal{A}}}/\Gamma_{\sigma^{\star}_{\mathcal{A}}\rightarrow\sigma_{\mathcal{B}}} = \Gamma_{\sigma_{\mathcal{B}}\rightarrow\sigma^{\star}_{\mathcal{C}}}/\Gamma_{\sigma^{\star}_{\mathcal{C}}\rightarrow\sigma_{\mathcal{B}}} = \exp[-\epsilon/(k_{\mathrm{B}}T)]$, again in accordance with detailed balance. Particularly important for the further discussion are the transition rates connecting the states $\sigma_{\mathcal{A}}$ and $\sigma^{\star}_{\mathcal{A}}$ or $\sigma_{\mathcal{C}}$ and $\sigma^{\star}_{\mathcal{C}}$, respectively, which for $\epsilon > 0$ are given by $\Gamma_{\sigma_{\mathcal{A}}\rightarrow\sigma^{\star}_{\mathcal{A}}} = \Gamma_{\sigma_{\mathcal{C}}\rightarrow\sigma^{\star}_{\mathcal{C}}} = \exp[-\epsilon/(k_{\mathrm{B}}T)]$ and $\Gamma_{\sigma^{\star}_{\mathcal{A}}\rightarrow\sigma_{\mathcal{A}}} = \Gamma_{\sigma^{\star}_{\mathcal{C}}\rightarrow\sigma_{\mathcal{C}}} = 1$, so that $\Gamma_{\sigma_{\mathcal{A}}\rightarrow\sigma^{\star}_{\mathcal{A}}}/\Gamma_{\sigma^{\star}_{\mathcal{A}}\rightarrow\sigma_{\mathcal{A}}} = \Gamma_{\sigma_{\mathcal{C}}\rightarrow\sigma^{\star}_{\mathcal{C}}}/\Gamma_{\sigma^{\star}_{\mathcal{C}}\rightarrow\sigma_{\mathcal{C}}} = \exp[-\epsilon/(k_{\mathrm{B}}T)]$. In all mentioned cases, k_{B} denotes Boltzmann's constant and T is the absolute temperature. Although the system under consideration is quite simple, an exact analytical treatment seems not to be feasible, particularly in the non-equilibrium case focused on below. Therefore, the following discussion relies on numerical simulations of the system dynamics [13]. The quantities of interest are the time dependent particle pair coordinate $x(t) = [x_1(t) + x_2(t)]/2$, in units of number of sites, for a particle pair being initially located at $x_1(t = 0) = 0$ and $x_2(t = 0) = 1$, where t denotes the number of time steps in units of attempted state changes, as well as the mean coordinate's probability distribution $P_t(x)$, where $P_t(x)\,\mathrm{d}x$ is the probability to find the particle pair between coordinate x and $x + \mathrm{d}x$ after t time steps. By calculating the first moment of the latter quantity, one obtains the mean distance $\overline{x}(t) = \int_{-\infty}^{\infty} x P_t(x)\,\mathrm{d}x$ after t time steps, from which the mean velocity $\overline{v}$ is calculated as the long-time limit $\overline{v} = \lim_{t\rightarrow\infty} \overline{x}(t)/t$.

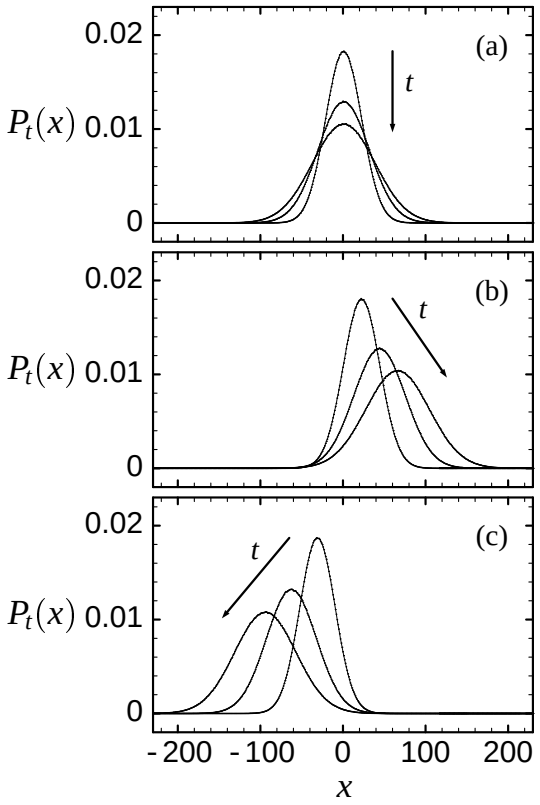

Fig. 2. Plot of the probability distribution function $P_t(x)$ *vs.* mean coordinate x of the particle pair, with $x = x(t) = [x_1(t) + x_2(t)]/2$, after t time steps for $\Delta/(k_{\mathrm{B}}T) = 1$, $\Delta'/(k_{\mathrm{B}}T) = 2$, $\epsilon/(k_{\mathrm{B}}T) = 1$, and (a) equilibrium case (corresponds to $\eta/(k_{\mathrm{B}}T) = 0$, pure diffusive motion), and non-equilibrium cases (b) $\eta/(k_{\mathrm{B}}T) = 1$ (biased motion to the right), and (c) $\eta/(k_{\mathrm{B}}T) = -1$ (biased motion to the left). In each subfigure, three different times are shown, $t = 10^4$, 2×10^4, and 3×10^4.

Before discussing the behavior of the system under non-equilibrium conditions, let me briefly mention the behavior of the system being in thermal equilibrium. Here, in particular when the probabilities $\Pi_{\sigma_{\mathcal{A}}}$, $\Pi_{\sigma^{\star}_{\mathcal{A}}}$, $\Pi_{\sigma_{\mathcal{C}}}$ and $\Pi_{\sigma^{\star}_{\mathcal{C}}}$ to be in the states $\sigma_{\mathcal{A}}$, $\sigma^{\star}_{\mathcal{A}}$, $\sigma_{\mathcal{C}}$, and $\sigma^{\star}_{\mathcal{C}}$, respectively, fulfill Boltzmann's law $\Pi_{\sigma^{\star}_{\mathcal{A}}}/\Pi_{\sigma_{\mathcal{A}}} = \Pi_{\sigma^{\star}_{\mathcal{C}}}/\Pi_{\sigma_{\mathcal{C}}} = \exp[-\epsilon/(k_{\mathrm{B}}T)]$, diffusive motion of the particle pair is observed, as one expects. In Figure 2a shown is

the corresponding probability distribution function $P_t(x)$, which is spatially symmetric around the particle pair's starting point and broadens with increasing number of time steps. It should be noted that such a diffusive motion of the particle pair is observed even in the case of the two barriers being different, $\Delta' \neq \Delta$, as it is indeed the case in Figure 2a.

3 Results

The following discussion focuses on the behavior of the system under non-equilibrium conditions resulting from over- and underpopulating the excited states $\sigma^\star_{\mathcal{A}}$ and $\sigma^\star_{\mathcal{C}}$, so that either $\Pi_{\sigma^\star_{\mathcal{A}}}/\Pi_{\sigma_{\mathcal{A}}} = \Pi_{\sigma^\star_{\mathcal{C}}}/\Pi_{\sigma_{\mathcal{C}}} > \exp[-\epsilon/(k_{\mathrm{B}}T)]$ (*i.e.* overpopulated) or $\Pi_{\sigma^\star_{\mathcal{A}}}/\Pi_{\sigma_{\mathcal{A}}} = \Pi_{\sigma^\star_{\mathcal{C}}}/\Pi_{\sigma_{\mathcal{C}}} < \exp[-\epsilon/(k_{\mathrm{B}}T)]$ (*i.e.* underpopulated). In the numerical simulation, the over- and underpopulation is done similarly to an actual experiment by 'pumping' the transitions $\sigma_{\mathcal{A}} \leftrightarrow \sigma^\star_{\mathcal{A}}$ and $\sigma_{\mathcal{C}} \leftrightarrow \sigma^\star_{\mathcal{C}}$ feeding energy into the system, which is numerically described herein by an energy parameter η. In the 'unpumped' equilibrium case ($\eta = 0$) fulfilling detailed balance, one has the transition rates $\Gamma_{\sigma_{\mathcal{A}}\to\sigma^\star_{\mathcal{A}}} = \Gamma_{\sigma_{\mathcal{C}}\to\sigma^\star_{\mathcal{C}}} = \exp[-\epsilon/(k_{\mathrm{B}}T)]$ and $\Gamma_{\sigma^\star_{\mathcal{A}}\to\sigma_{\mathcal{A}}} = \Gamma_{\sigma^\star_{\mathcal{C}}\to\sigma_{\mathcal{C}}} = 1$ between the respective two states, as discussed above. These four rates are replaced in the case of 'pumping' by four new generalized transition rates, either by: (i) $\tilde{\Gamma}_{\sigma_{\mathcal{A}}\to\sigma^\star_{\mathcal{A}}} = \tilde{\Gamma}_{\sigma_{\mathcal{C}}\to\sigma^\star_{\mathcal{C}}} = \exp[-(\epsilon+\eta)/(k_{\mathrm{B}}T)]$ and $\tilde{\Gamma}_{\sigma^\star_{\mathcal{A}}\to\sigma_{\mathcal{A}}} = \tilde{\Gamma}_{\sigma^\star_{\mathcal{C}}\to\sigma_{\mathcal{C}}} = 1$ for $\eta \geq 0$ or (ii) $\tilde{\Gamma}_{\sigma_{\mathcal{A}}\to\sigma^\star_{\mathcal{A}}} = \tilde{\Gamma}_{\sigma_{\mathcal{C}}\to\sigma^\star_{\mathcal{C}}} = \exp[-\epsilon/(k_{\mathrm{B}}T)]$ and $\tilde{\Gamma}_{\sigma^\star_{\mathcal{A}}\to\sigma_{\mathcal{A}}} = \tilde{\Gamma}_{\sigma^\star_{\mathcal{C}}\to\sigma_{\mathcal{C}}} = \exp[\eta/(k_{\mathrm{B}}T)]$ for $\eta \leq 0$. The reason for treating the cases $\eta \geq 0$ and $\eta \leq 0$ separately is to ensure that $\tilde{\Gamma}_{\sigma^\star_{\mathcal{A}}\to\sigma_{\mathcal{A}}} \leq 1$, $\tilde{\Gamma}_{\sigma_{\mathcal{A}}\to\sigma^\star_{\mathcal{A}}} \leq 1$, $\tilde{\Gamma}_{\sigma^\star_{\mathcal{C}}\to\sigma_{\mathcal{C}}} \leq 1$, and $\tilde{\Gamma}_{\sigma_{\mathcal{C}}\to\sigma^\star_{\mathcal{C}}} \leq 1$ $\forall\eta$. In both cases (i) and (ii), one gets $\tilde{\Gamma}_{\sigma_{\mathcal{A}}\to\sigma^\star_{\mathcal{A}}}/\tilde{\Gamma}_{\sigma^\star_{\mathcal{A}}\to\sigma_{\mathcal{A}}} = \tilde{\Gamma}_{\sigma_{\mathcal{C}}\to\sigma^\star_{\mathcal{C}}}/\tilde{\Gamma}_{\sigma^\star_{\mathcal{C}}\to\sigma_{\mathcal{C}}} = \exp[-(\epsilon+\eta)/(k_{\mathrm{B}}T)]$, so that $\eta > 0$ results in underpopulating the excited states $\sigma^\star_{\mathcal{A}}$ and $\sigma^\star_{\mathcal{C}}$, whereas $\eta < 0$ yields overpopulating.

When performing numerical simulations for $\eta \neq 0$, in the case of identical barriers $\Delta' = \Delta$ one nevertheless observes a diffusive motion of the particle pair, *i.e.* a mean velocity $\overline{v} = 0$, as the spatial symmetry of the excited states is not broken. The resulting probability distribution function $P_t(x)$ is quite similar to the one shown in Figure 2a. For the case $\Delta' \neq \Delta$, however, a *directed* transport of the particle pair is observed for $\eta \neq 0$. For example in the case $\Delta' > \Delta$, one obtains a mean velocity $\overline{v} > 0$ when underpopulating the excited states $\sigma^\star_{\mathcal{A}}$ and $\sigma^\star_{\mathcal{C}}$ by $\eta > 0$ (see Fig. 2b), and a mean velocity $\overline{v} < 0$ when overpopulating the excited state $\sigma^\star_{\mathcal{A}}$ and $\sigma^\star_{\mathcal{C}}$ by $\eta < 0$ (see Fig. 2c). In the opposite case $\Delta' < \Delta$, one gets the inverse behavior: A mean velocity $\overline{v} < 0$ results for $\eta > 0$, whereas $\eta < 0$ yields a mean velocity $\overline{v} > 0$.

The actual value of the mean velocity $\overline{v}$ for given ϵ, Δ, and Δ' is determined by the amount of over- resp. underpopulation, *i.e.* by the value of η, as shown in Figure 3. Therefore, both the direction and the mean velocity of the particle pair's motion can be chosen dynamically.

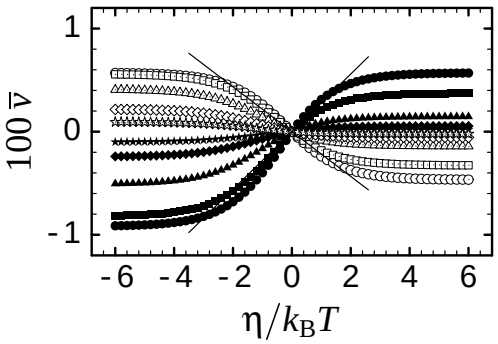

Fig. 3. Plot of the mean velocity $\overline{v}$ *vs.* bias η for $\Delta/(k_{\mathrm{B}}T) = 1$ and $\Delta'/(k_{\mathrm{B}}T) = 2$ (full symbols) and $\Delta/(k_{\mathrm{B}}T) = 2$ and $\Delta'/(k_{\mathrm{B}}T) = 1$ (open symbols). The results are obtained for $\epsilon/(k_{\mathrm{B}}T) = 1/2$ (circles), $\epsilon/(k_{\mathrm{B}}T) = 1$ (squares), $\epsilon/(k_{\mathrm{B}}T) = 2$ (triangles), $\epsilon/(k_{\mathrm{B}}T) = 3$ (diamonds), and $\epsilon/(k_{\mathrm{B}}T) = 4$ (stars). The two lines indicate fits in the linear response regime for the case $\epsilon/(k_{\mathrm{B}}T) = 1$ (squares), with $\overline{v} \cong 0.003\eta/(k_{\mathrm{B}}T)$ and $\overline{v} \cong -0.002\eta/(k_{\mathrm{B}}T)$ for $|\eta|/(k_{\mathrm{B}}T) < 0.7$.

This means that, although the system's symmetry is broken statically by choosing either $\Delta' > \Delta$ or $\Delta' < \Delta$, one can benefit in two different manners from this broken symmetry. It is important to note that there exists a linear response regime in which $\overline{v}$ depends linearly on η, which is generic of ratchet-type models [11]. For example for the value $\epsilon/(k_{\mathrm{B}}T) = 1$, for the case $\Delta/(k_{\mathrm{B}}T) = 1$ and $\Delta'/(k_{\mathrm{B}}T) = 2$, linear response $\overline{v} \cong 0.003\,\eta/(k_{\mathrm{B}}T)$ holds for $|\eta|/(k_{\mathrm{B}}T) < 0.7$, see Figure 3. Analogously, for the inverse case $\Delta/(k_{\mathrm{B}}T) = 2$ and $\Delta'/(k_{\mathrm{B}}T) = 1$, linear response $\overline{v} \cong -0.002\,\eta/(k_{\mathrm{B}}T)$ holds for the same range of values for η. Therefore, the slight asymmetry observed when comparing Figures 2b and c origins in the fact that the values $\eta/(k_{\mathrm{B}}T) = \pm 1$ used in the figures are outside the linear response regime.

The discussion so far has concentrated on the case in which $\sigma^\star_{\mathcal{A}}$ and $\sigma^\star_{\mathcal{C}}$ are really *excited* states meaning that they are *higher* in potential energy when compared to the other four states, *i.e* $\epsilon > 0$. However, the model under discussion can easily be generalized to the case $\epsilon = 0$ or even $\epsilon < 0$. The latter case means that the states $\sigma^\star_{\mathcal{A}}$ and $\sigma^\star_{\mathcal{C}}$ are *lower* in potential energy when compared to the other four states. Concerning the resulting transitions, for example for the states $\sigma_{\mathcal{B}}$ and $\sigma^\star_{\mathcal{A}}$ or $\sigma_{\mathcal{B}}$ and $\sigma^\star_{\mathcal{C}}$, respectively, the interconnecting transition rates for $\epsilon \leq 0$ are given by $\Gamma_{\sigma_{\mathcal{B}}\to\sigma^\star_{\mathcal{A}}} = \Gamma_{\sigma_{\mathcal{B}}\to\sigma^\star_{\mathcal{C}}} = \exp[-\Delta/(k_{\mathrm{B}}T)]$ and $\Gamma_{\sigma^\star_{\mathcal{A}}\to\sigma_{\mathcal{B}}} = \Gamma_{\sigma^\star_{\mathcal{C}}\to\sigma_{\mathcal{B}}} = \exp[-(\Delta-\epsilon)/(k_{\mathrm{B}}T)]$, so that $\Gamma_{\sigma^\star_{\mathcal{A}}\to\sigma_{\mathcal{B}}}/\Gamma_{\sigma_{\mathcal{B}}\to\sigma^\star_{\mathcal{A}}} = \Gamma_{\sigma^\star_{\mathcal{C}}\to\sigma_{\mathcal{B}}}/\Gamma_{\sigma_{\mathcal{B}}\to\sigma^\star_{\mathcal{C}}} = \exp[\epsilon/(k_{\mathrm{B}}T)]$. Analogously, the transitions connecting $\sigma_{\mathcal{A}}$ and $\sigma^\star_{\mathcal{A}}$ or $\sigma_{\mathcal{C}}$ and $\sigma^\star_{\mathcal{C}}$, respectively, are given by (i) $\tilde{\Gamma}_{\sigma^\star_{\mathcal{A}}\to\sigma_{\mathcal{A}}} = \tilde{\Gamma}_{\sigma^\star_{\mathcal{C}}\to\sigma_{\mathcal{C}}} = \exp[-(\eta-\epsilon)/(k_{\mathrm{B}}T)]$ and $\tilde{\Gamma}_{\sigma_{\mathcal{A}}\to\sigma^\star_{\mathcal{A}}} = \tilde{\Gamma}_{\sigma_{\mathcal{C}}\to\sigma^\star_{\mathcal{C}}} = 1$ for $\eta \geq 0$ or (ii) $\tilde{\Gamma}_{\sigma^\star_{\mathcal{A}}\to\sigma_{\mathcal{A}}} = \tilde{\Gamma}_{\sigma^\star_{\mathcal{C}}\to\sigma_{\mathcal{C}}} = \exp[\epsilon/(k_{\mathrm{B}}T)]$ and $\tilde{\Gamma}_{\sigma_{\mathcal{A}}\to\sigma^\star_{\mathcal{A}}} = \tilde{\Gamma}_{\sigma_{\mathcal{C}}\to\sigma^\star_{\mathcal{C}}} = \exp[\eta/(k_{\mathrm{B}}T)]$ for $\eta \leq 0$. This generalization allows to study the dependence of the maximum velocity $\overline{v}_{\max} = \lim_{\eta\to-\infty}\overline{v}$ for maximal overpopulation or $\overline{v}_{\max} = \lim_{\eta\to\infty}\overline{v}$ for maximal underpopulation on the energy difference ϵ for both $\epsilon \geq 0$ and $\epsilon \leq 0$, the results

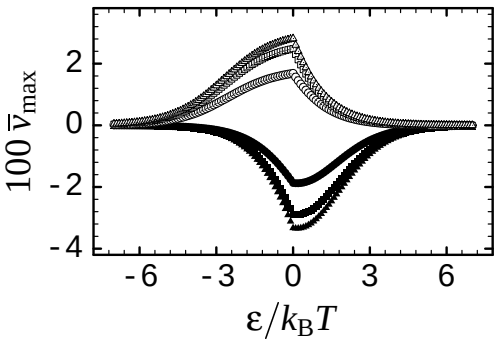

Fig. 4. Plot of the maximum velocity $\overline{v}_{\max}$ *vs.* energy ϵ for $\eta/(k_{\mathrm{B}}T) = -20$ (full symbols) and $\eta/(k_{\mathrm{B}}T) = 20$ (open symbols). The different symbols correspond to $\Delta/(k_{\mathrm{B}}T) = 1$ and $\Delta'/(k_{\mathrm{B}}T) = 2$ (circles), $\Delta/(k_{\mathrm{B}}T) = 1$ and $\Delta'/(k_{\mathrm{B}}T) = 3$ (squares), and $\Delta/(k_{\mathrm{B}}T) = 1$ and $\Delta'/(k_{\mathrm{B}}T) = 4$ (triangles).

are shown in Figure 4. For given values of Δ and Δ', a resonance-like behavior as a function of ϵ is observed. The maximum velocity $\overline{v}_{\max}$ shows a maximum at $\epsilon = 0$ and drops to zero for $|\epsilon| \gg \max\{\Delta, \Delta'\}$. The reason for the best performance being observed for vanishing energy difference is, that in this case the equilibrium probabilities to be in the states $\sigma_{\mathcal{A}}$, $\sigma_{\mathcal{C}}$, $\sigma^{\star}_{\mathcal{A}}$, and $\sigma^{\star}_{\mathcal{C}}$ are equal and hence the over- and underpopulating can draw the best benefit from the difference between the two barriers Δ and Δ'.

Concerning a second generalization it should be noted that the model can be reformulated by using four different barriers Δ_1, $\Delta_1^{\star}$, Δ_2, and $\Delta_2^{\star}$ instead of the two barriers Δ and Δ'. Here, Δ_1 and $\Delta_1^{\star}$ are the barriers particle 1 has to overcome when leaving or entering the states $\sigma_{\mathcal{A}}$ and $\sigma_{\mathcal{C}}$ or $\sigma^{\star}_{\mathcal{A}}$ and $\sigma^{\star}_{\mathcal{C}}$, respectively. Analogously, particle 2 has to overcome the barriers Δ_2 and $\Delta_2^{\star}$ when leaving or entering the states $\sigma_{\mathcal{A}}$ and $\sigma_{\mathcal{C}}$ or $\sigma^{\star}_{\mathcal{A}}$ and $\sigma^{\star}_{\mathcal{C}}$, respectively. The above discussion has concentrated on the case $\Delta_1 = \Delta_1^{\star} = \Delta_2 = \Delta$ and $\Delta_2^{\star} = \Delta'$. It should be noted that in the general case of four different barriers, directed transport is observed for $\Delta_1 \neq \Delta_1^{\star}$ and $\Delta_2 = \Delta_2^{\star}$ or $\Delta_2 \neq \Delta_2^{\star}$ and $\Delta_1 = \Delta_1^{\star}$. In the case that both $\Delta_1 \neq \Delta_1^{\star}$ and $\Delta_2 \neq \Delta_2^{\star}$, a general answer whether directed transport occurs or not is difficult to give and depends on the actual barrier values. For example, directed transport is observed for $\Delta_1 < \Delta_1^{\star}$ and $\Delta_2 > \Delta_2^{\star}$, but not for $\Delta_1 = \Delta_2$ and $\Delta_1^{\star} = \Delta_2^{\star}$.

4 Conclusions

In summary, it has been shown that a pair of bounded particle can show a directed motion in the asymmetric case of the system dynamics including excited states which differ from the respective ground states by the barrier to be overcome by one of the two particles. The directed motion is caused and controlled by an externally driven over- resp. underpopulation of these excited system states. For small deviations from equilibrium, the system shows a linear response well known from other ratchet-type models [11].

Concerning possible applications of the proposed concept, in particular to machinery on the mesoscopic to nanometer scale, it is important to stress two points: (i) The discussed directed transport is only one example of one specific purpose of such a machine. As the discussion has been done in the general context of system states and random transitions between them, any other purpose is possible by assigning a different meaning to what is called 'left' and 'right' herein. (ii) The 'pumping' of the transitions $\sigma_{\mathcal{A}} \leftrightarrow \sigma^{\star}_{\mathcal{A}}$ and $\sigma_{\mathcal{C}} \leftrightarrow \sigma^{\star}_{\mathcal{C}}$ does not need necessarily to be done by physical means such as for example by light, but might also be supplied chemically by some kind of 'fuel,' similarly as the non-equilibrium chemical reaction adenosine triphosphate (ATP) to adenosine diphosphate (ADP) drives motor proteins in biological systems.

Helpful comments on the manuscript by A. Ordemann are gratefully acknowledged.

References

1. Special Issue 5408, *Frontiers in Chemistry: Single Molecules*, Science **283**, 1667–1695 (1999).
2. See for example (i) *supramolecular structures such as catenanes and rotaxanes*: V. Balzani, M. Gómez-López, J.F. Stoddard, Acc. Chem. Res. **31**, 405 (1998); J.-P. Sauvage, Acc. Chem. Res. **31**, 611 (1998); N. Armaroli *et al.*, J. Am. Chem. Soc. **121**, 4397 (1999); G. Schill, *Catenanes, Rotaxanes, and Knots* (Academic Press, New York, 1971); M.C. Jiménez, C. Dietrich-Buchecker, J.-P. Sauvage, Angew. Chem. Int. Edn. **39**, 3284 (2000); A.M. Brouwer *et al.*, Science **291**, 2124 (2001); (ii) *molecular rotors*: T.R. Kelly, H. De Silva, R.A. Silva, Nature (London) **401**, 150 (1999); N. Koumura *et al.*, Nature (London) **401**, 152 (1999); T.R. Kelly *et al.*, J. Am. Chem. Soc. **122**, 6935 (2000); (iii) *a DNA based and fuelled machine*: B. Yurke *et al.*, Nature (London) **406**, 605 (2000); F.C. Simmel, B. Yurke, Phys. Rev. E **63**, 041913 (2001); (iv) *a hybrid machine based on F_1-ATPase*: R.K. Soong *et al.*, Science **290**, 1555 (2000).
3. After the field has been established in 1992/93 (*cf.* A. Ajdari, J. Prost, C.R. Acad. Sci., Ser. II: Mec., Phys., Chim., Sci. Terre Univers **315**, 1635 (1992) and M.O. Magnasco, Phys. Rev. Lett. **71**, 1477 (1993), to mention only the first two papers), a large amount of literature has accumulated, so that it is almost impossible to give a short yet balanced list of references covering the whole area. Therefore, the reader is refered to the review P. Reimann, Phys. Rep. (in print), see `cond-mat/0010237`, for a very comprehensive list of references.
4. K.W. Kehr, K. Mussawisade, T. Wichmann, W. Dieterich, Phys. Rev. E **56**, R2351 (1997) and Physica Status Solidi B **205**, 73 (1998); L. Schimansky-Geier, M. Kschischo, T. Fricke, Phys. Rev. Lett. **79**, 3335 (1997); A.B. Kolomeisky, B. Widom, J. Stat. Phys. **93**, 633 (1998); I.M. Sokolov, J. Phys. A **32**, 2541 (1999); J.A. Freund, L. Schimansky-Geier, Phys. Rev. E **60**, 1304 (1999); K.W. Kehr, Z. Koza, Phys. Rev. E **61**, 2319 (2000); J.M.R. Parrondo, G.P. Harmer, D. Abbott, Phys. Rev. Lett. **85**, 5226 (2000); B. Cleuren, C. van den Broeck, Europhys. Lett. **54**, 1 (2001); M. Porto, Phys. Rev. E **64**,

021109 (2001); for an investigation of velocity and diffusion constant in a periodic one-dimensional system in a different context see B. Derrida, J. Stat. Phys. **31**, 433 (1983); for a detailed discussion and comparison with continuous models, the reader is refered likewise to the review of reference [3].

5. J. Howard, Nature (London) **389**, 561 (1997); F. Jülicher, A. Ajdari, J. Prost, Rev. Mod. Phys. **69**, 1269 (1997); A. Huxley, Nature (London) **391**, 239 (1998); J. Howard, Nature (London) **391**, 240 (1998); Y. Okada, N. Hirokawa, Science **283**, 1152 (1999).
6. A. Ajdari, J. Phys. I France **4**, 1577 (1994).
7. I. Derényi, T. Vicsek, Proc. Natl. Acad. Sci. (USA) **93**, 6775 (1996).
8. A. Mogilner, M. Mangel, R.J. Baskin, Phys. Lett. A **237**, 297 (1998).
9. G.N. Stratopoulos, T.E. Dialynas, G.P. Tsironis, Phys. Lett. A **252**, 151 (1999).
10. M. Porto, M. Urbakh, J. Klafter, Phys. Rev. Lett. **84**, 6058 (2000); *ibid* **85**, 491 (2000); M. Porto, Phys. Rev. E **63**, 030102(R) (2001).
11. A. Parmeggiani, F. Jülicher, A. Ajdari, J. Prost, Phys. Rev. E **60**, 2127 (1999).
12. See for example R. Kutner, D. Knödler, P. Penzig, R. Przenioslo, W. Dieterich, in *Diffusion Processes: Experiment, Theory, Simulations*, edited by A. Pekalski, Lect. Notes Phys., Vol. 438 (Springer, Berlin, 1994), pp. 197; K.W. Kehr, K. Mussawisade, T. Wichmann, in *Diffusion in Condensed Matter*, edited by J. Kärger, P. Heitjans, R. Haberlandt (Vieweg Verlag, Braunschweig, 1998), pp. 265.
13. To perform the numerical simulation, the system is put in state $\sigma_{\mathcal{A}}$ at time $t = 0$, and the particles' coordinate are set to $x_1(t = 0) = 0$ and $x_2(t = 0) = 1$. Then, in each time step t, for the system being in state $u \in \{\sigma_{\mathcal{A}}, \sigma_{\mathcal{B}}, \sigma_{\mathcal{C}}, \sigma_{\mathcal{D}}, \sigma^{\star}_{\mathcal{A}}, \sigma^{\star}_{\mathcal{C}}\}$ at first one of states v connected to u by a direct transition is chosen randomly with equal probability. Secondly, the transition to state v is performed with probability $\Gamma_{u\to v}$, whereas with probability $1 - \Gamma_{u\to v}$ the system remains in state u. In any case the particles' coordinates $x_1(t)$ and $x_2(t)$ are updated accordingly from the former coordinates $x_1(t-1)$ and $x_2(t-1)$. After a certain large number of time steps, the particles' positions are obtained. The whole simulation is repeated, and an ensemble average is performed over a large number of 10^8 independent configurations.